Journal of Ceramic Processing Research. Vol. 24, No. 2, pp. 367~373 (2023)
(Received 3 August 2022, Received in revised form 27 August 2022, Accepted 26 September 2022)
https://doi.org/10.36410/jcpr.2023.24.2.367

J O U R N A L O F
Ceramic Processing Research

Effect of ethylene glycol on the synthesis of crystalline boron carbide powder from condensed boric-acid-glycerin precursor

Li Yang[a,b], Li Sanxi[b,*], Wang Song[b], Tian Chengcheng[a,b] and Otitoju Tunmise Ayode[a,b]
[a]*School of Materials Science and Engineering, Shenyang University of Technology, Liaoning 110870, China*
[b]*School of Environmental and Chemical Engineering, Shenyang University of Technology, Liaoning 110870, China*

The effect of addition of ethylene glycol ($C_2H_6O_2$) on the synthesis of crystalline boron carbide (B_4C) powder from a condensed boric acid (H_3BO_3)-glycerin ($C_3H_8O_3$) product was investigated. Equal molar amount of H_3BO_3 and glycerin was mixed and subjected to dehydration-condensation reaction using various amount of ethylene glycol (0 to 40 mol% based on glycerol amount). Then the condensed product was thermally decomposed in air twice to obtain surface carbon-free precursor powder. The crystalline phases and surface functional groups of the material was characterized using XRD, SEM, FTIR and TGA. Addition of ethylene glycol offered a new organic sites and comparatively, reduced pyrolysis temperature from 700 to 650 °C. The complete formation of crystalline B_4C powder was achieved at 1475 °C within 2.5 h, which is among the shortest time reported for B_4C synthesis.

Keywords: Boron carbide, Glycerin, Dehydration-condensation reaction, Shortest time.

Introduction

Boron carbide (B_4C) is a vital non-oxide ceramic with excellent properties. The atomic structure of B_4C is rather unique. The primary structural units of boron carbide are 12-atom icosahedra and the 3-atom linear chains, and its high melting point, high-modulus, outstanding thermal stability, excellent hardness (35-45 GPa), low density (2.52 $g \cdot cm^{-3}$), high neutron absorption cross-section and remarkable chemical inertness [1-5] confers on it a material of choice for a wide range of engineering applications [1-3]. Boron carbide is widely used in grinding hard materials, lightweight bullet-proof armor, advanced refractories, shielding materials of nuclear reactor an, rocket solid fuel and many other areas. Several synthesis methods have been adopted to produce B_4C powder [5, 6], namely, carbothermal reduction [7], synthesis from precursor elements [8], self–propagation high temperature synthesis (SHS) [9], laser-induced chemical vapor deposition (LICVD) [10], and mechanical alloying process [11].

In carbothermal reduction process for B_4C powder production, boron oxide (B_2O_3) and carbon black or petroleum coke are reduced in an electric furnace as represented in Equation (1). Many commercial production of B_4C utilize carbothermal reduction process because of the inexpensive and nonhazardous nature of the raw materials. However, this process presents some drawbacks such as loss of B_2O_3 by volatilization and the final product contains a free-carbon residue. Also, the final B_4C obtained is coarse, which is caused primarily by the high synthesis temperature (approximately 2000 °C) [12]. Thus, energy-intensive grinding is usually required to reduce the particle size to powder.

$$2B_2O_3(s) + 7C(s) \rightarrow B_4C(s) + 6CO(g) \quad (1)$$

Boric acid (H_3BO_3) as the boron source, and polyols such as poly (vinyl alcohol) (PVA) [13-15], cellulose [16], glucose and starch [24], citric acid [17], glycerin [18, 19], phenolic resin [20], sucrose [21], mannitol [22] as carbon source have been utilized to produce B_4C powder. The dehydration-condensation reaction of boric acid and polyols as a carbon source before carbothermal reduction avails the opportunity of manipulating the interactions of the precursors from molecular level perspective. The B-O-C bond formed from the condensation reaction enables homogeneous dispersion of the boron and carbon, which can result in lower synthesis temperature (approximately 1500 °C). Also, precise adjustment of the chemical composition of the gel precursor to meet the requirements of optimized properties for task specific B_4C products can be achieved in this stage [20, 23]. However, the challenges of residual free carbon that affects the final B_4C is much evident. In an attempt to remove the free residual carbon, in our previous study, the thermal decomposition in air was employed to remove the excess amount of carbon.

In this study, various amount of ethylene glycol was added to investigate the effect on condensed H_3BO_3-

*Corresponding author:
Tel : +86 18704009103
E-mail: lisx@sut.edu.cn

glycerin product and dehydration-condensation reaction temperature. The ethylene glycol with its two hydroxyl groups offer new sites that could possibly reduce dehydration-condensation temperature and increase the uniform dispersion of carbon and boron. Also, the best boric acid-glycerin-ethylene glycol ratio for pyrolysis of precursor and reaction influencing parameters were determined.

Experimental

Synthesis of B_4C powder

Boric acid [H_3BO_3 (BA), 99.5%], glycerin ($C_3H_8O_3$, 99.0%), ethylene glycol [$C_2H_6O_2$ (EG), 99.5%], were purchased from Guoyao Group Chemical Reagent Shenyang Co., Ltd. The synthesis of B_4C powder were carried out according to ref. with slight modification. The condensed product was prepared via dehydration-condensation reaction of equimolar boric acid (denoted as BA) and glycerin (GA) and various amount of ethylene glycol (EG) (typically 0 to 40 mol% based on glycerol amount). First, the EG and GA solution was heated at various temperature range of 80 ºC to 120 ºC under vigorous stirring. Then BA was added to the solution containing GA and EG. The resulting mixture was brought to 150 ºC for 2.5 h. The condensed product were placed in alumina crucible and heated in air at 250 ºC for 2 h and then at 350 ºC for another 2 h. The above steps were consecutively performed at a heating rate of 5 ºC/min using a PID temperature controlled muffle furnace. The obtained black solid was ground into powder with an agate mortar, followed by thermal decomposition in air at temperature range of 550 to 700 ºC for 2 h. The precursor powder obtained after thermal decomposition were labeled as P0 to P4 according to amount of EG added. The carbothermal reduction of the precursor sample were carried out in a graphite boat under Ar flow (200 mL/min) at 1475 ºC and heating rate of 10 ºC/min for 2.5 h.

Characterization

The surface functional groups of the raw materials and condensed products were obtained using Fourier transform infrared (FT-IR) (Shimadzu IR Prestige-21 spectrometer). The samples were prepared using KBr pellet technique over a scanning range of 4000 to 40 cm^{-1} and a resolution of 4 cm^{-1}. Thermogravimetric analysis of the raw materials and condensed products were performed using Rigaku Thermo Plus TG8120 under nitrogen from 0 ºC to 700 ºC at heating scan of 10 ºC/min. The scanning electron microscopy (SEM) observations of the morphologies of the precursor and product powders were conducted with a Hitachi SU8010 field-emission scanning electron microscope operated at 15 kV. Prior to SEM analysis, the samples were coated with 5 nm-thick Pt-Pd. The particle size distribution of the product powders was determined from the SEM images. Powdered X-ray diffraction (XRD) were conducted using Rigaku RAD-C, to reveal the amorphous and crystalline phases of the precursor and product powders. The X-ray diffractometer was operated at 40 kV/30 mA under monochromatized Cu Kα radiation. The B_4C peak intensity ratio [$I_{B4C}/(I_{B4C} + I_C + I_{B2O3})$] of the products was estimated from the main peak intensities of each of the B_4C [I_{B4C}: (021) reflection at 2 h = 37.8], carbon (I_C; amorphous halo at 2 h = 23-27), and B_2O_3 [I_{B2O3}: (031) reflection at 2 h = 27.8] components in the XRD pattern. Three B_4C peak intensity ratios were estimated for each product to ensure consistency in the formation behavior of the B_4C.

Table 1. The diffraction peak intensity ratio of B_4C of final products with 0-40% EG.

Ethylene glycol/%	I_{B_4C} /a.u	I_C /a.u	$I_{B_4C}/(I_{B_4C}+I_C+I_{B_2O_3})$
0	6393	–	1.000
10	4834	637	0.884
20	9079	–	1.000
30	4343	950	0.821
40	6393	1567	1.000

Results and Discussion

FT-IR analysis of the raw materials, condensed and pyrolized products

The dehydration condensation reaction is induced by heating amixture of GL and BA dissolved in 0-40 mol% EG at 160 ºC. In order to comprehend the formation of borate ester, FT-IR measurement was performed to evaluate the bonding state of the condensed products. The FT-IR spectra of the starting materials and the condensed products with different amounts of GL added are shown in Figs. 1 and 2, respectively. The absorption peaks assigned to the C-O stretching mode

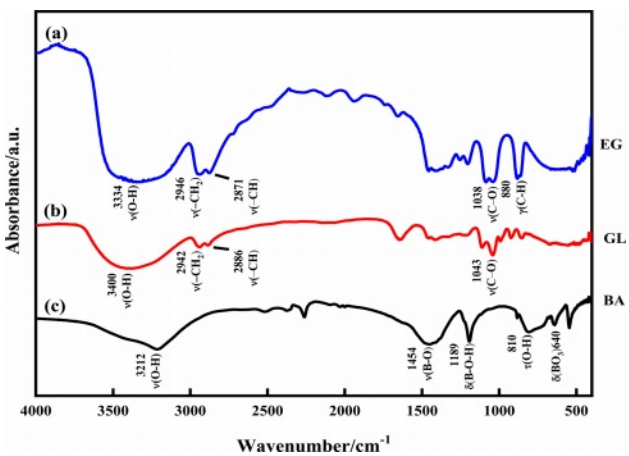

Fig. 1. FT-IR spectra of (a) EG, (b) GL, and (c) BA.

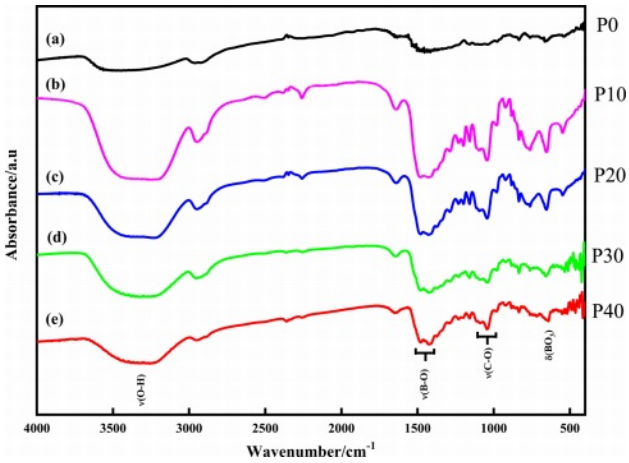

Fig. 2. FT-IR spectra of condensed products with (a) 0 mol%, (b) 10 mol%, (c) 20 mol%, (d) 30 mol%, and (e) 40 mol% EG added.

at 950-1150 cm^{-1} and to the B-O stretching mode at 1300-1500 cm^{-1} [18, 24] were observed for the condensed product without EG added (Fig. 2(a)); these two peaks were derived from the starting materials GL and BA (Fig. 1(b) and (c), respectively). In contrast, the O-H stretching band at 3000-3500 cm^{-1} was relatively weaker than those of the starting materials, and the B-O-H bending band at 1195 cm^{-1} and the O-H torsion band at 752 cm^{-1} [18, 19, 25] derived from BA (Fig. 1(c)) disappeared in Fig. 2(a). These results indicate that borate ester (B-O-C) bonds were formed in the prepared condensed product by the dehydration condensation of BA and GL. It has been reported that a borate ester compound of glycerin has a polymeric structure, which is alternately crosslinked between BA and GL[10, 20]. Moreover, no B-O-H bending and O-H torsion bands derived from BA are observed in these spectra. These mean that hydroxyl groups of GL and EG that cannot react with BA exist in the condensed products with EG added.

TG analysis of the raw materials and condensed products

The TG profile of the raw materials presented in Fig. 3(a) showed that glycerol started decomposing around 110 ºC and plateaued at 150 ºC, leaving about 4% carbon residue, which is in the glycerol structure. Comparably, ethylene glycol, which is a dihydroxyl alcohol showed a higher decompose temperature. The first step from 200 to 320 ºC is associated to dehydration and liberation of the ethylene glycol structural water. Then the second step from 320 to 410 ºC is ascribed to thermal cracking of the carbon-carbon double bond. Hence, constant weight loss was achieved at 410 ºC. The structural water in the boric acid decomposed above 150 ºC leaving boric oxide. The boric oxide, which is the residual compound of boric acid decomposition, could sustain about 56% of the total mass above 200 ºC.

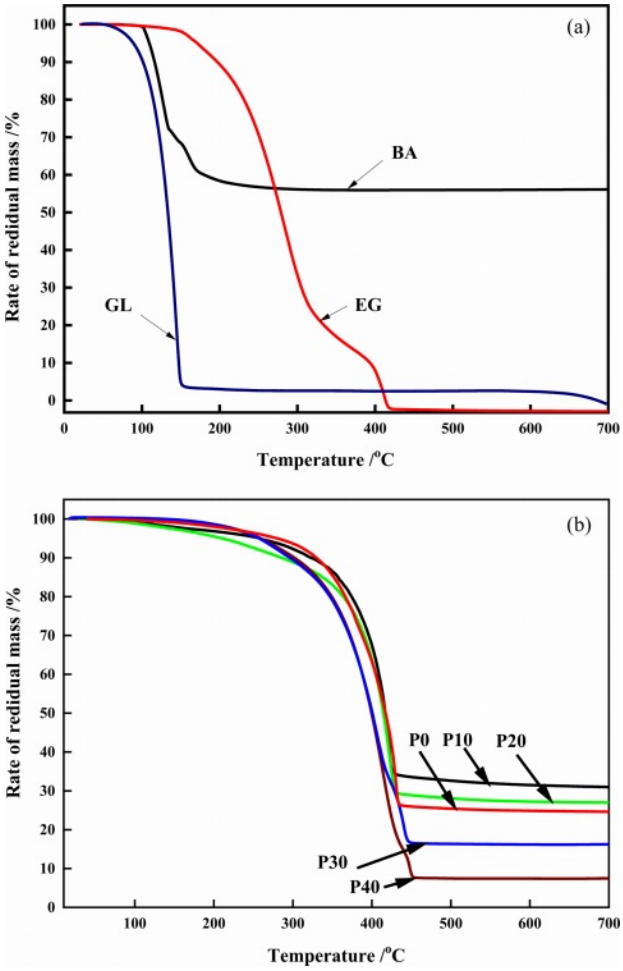

Fig. 3. TGA curves of raw materials (a) and polymeric precursors (b).

The condensed products at various ethylene glycol amount decomposition is shown in Fig. 3(b). The weight loss about 10% at 150 °C to 300 °C, is associated to the evaporation of the free water molecules in the organic precursor. It is worth noting that when only boron oxide and free carbon remain in the pyrolysis product, the pyrolysis reaction reaches the end point, and the quality of the remaining product no longer changes. As the temperature continues to increase, the carbon network structure is still changing, which is an important reason for the different morphology and size of the subsequent reduction products [19]. The second steep weight loss from 350 to 440 ºC is due to the fractured skeleton of six membered ring of the organic precursor. At 10 mol% (P10) ethylene glycol (35% residual mass loss), the residual mass loss was in orders of 5% lower than the sample (P0) without ethylene glycol (30% residual mass loss). As the ethylene glycol concentration increases from 20 mol% to 40 mol%, the residual percentage weight loss, suggesting that ethylene glycol addition propagates the esterification reaction that increases the organic phase. Hence, 40 mol% achieved constant weight loss (with

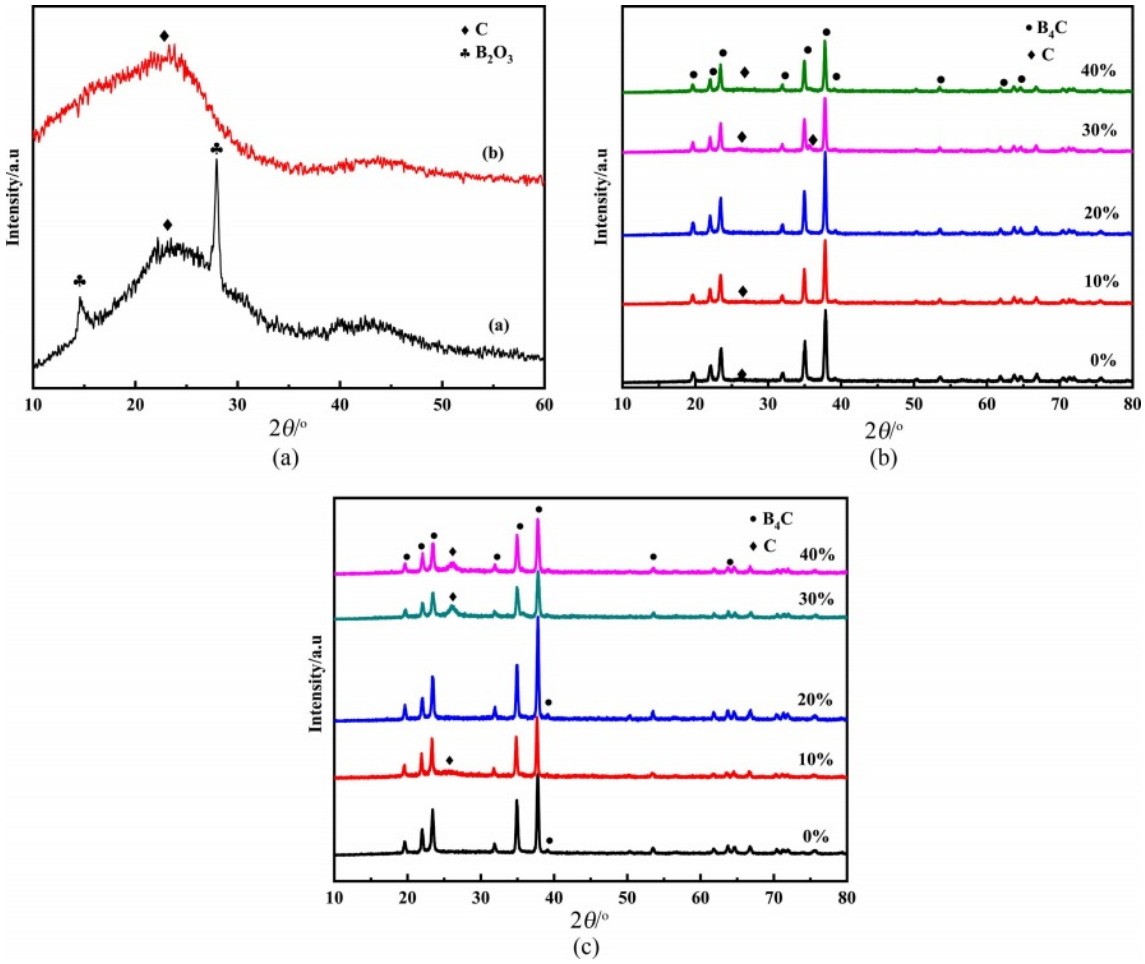

Fig. 4. (a) XRD patterns of (a) pyrolyzed precursor and (b) after product washing, (b) XRD patterns of the products (with 0-40% EG, 650 °C), (c) XRD patterns of the products (with 0-40% EG, 700 °C).

7.5% residue) at higher decomposition temperature around 450 °C. Constant weight loss was achieved in all the samples around 450 °C indicating that the thermal cracking reaction occurred at or below this temperature.

XRD analysis

The precursor (a) was heated at 250 °C for 2 h and then stored at 350 °C for 2 h. Then the XRD diagram of the pyrolysis product was obtained after holding 2 h at 650 °C. In the diagram (b), the XRD diagram of the residue obtained after washing the product with hot water was obtained. In Fig. 4(a), at 2θ = 14.6° and 2θ = 27.9° at low, but the peak sharp diffraction peak corresponding to the characteristic diffraction peaks of B_2O_3 crystal. The wide peak appeared in the 2θ = 23°-27° of diffraction peaks of free carbon, no characteristic diffraction peaks of B_4C crystal. Therefore, cracking product containing B_2O_3 and free carbon, B_4C does not exist, and the infrared spectra analysis of pyrolysis products. In order to further determine the composition of pyrolysis products, get the XRD figure with hot distilled water washing of pyrolysis products (b) are shown. Using hot distilled water after washing, XRD has no characteristic diffraction peaks of B_2O_3 crystal, only the diffraction peaks of free carbon wide was found in 2θ = 23-27°, at the same time no characteristic diffraction peaks of B_4C, that the only remaining free carbon residue after washing with hot water. It is shown that the composition of the pyrolysis products after two cryogenic cracking is B_2O_3 and free carbon.

The organic precursor was grinded after the first low temperature cracking, then cracked at 2 h at 650 °C, and then grinded into powder. The XRD diagram of the final product was obtained after holding 2.5 h at 1475 °C. But if the amount of ethylene glycol in 20%, under the same conditions of synthesis of the most pure B_4C, no diffraction peaks of free carbon. When ethylene glycol addition is 10%, the free carbon in B_4C, may be 10% glycol added amount is too small, not enough to affect the free carbon and B_2O_3 the distribution, but not with the addition of ethylene glycol synthesis after the final product of the XRD phase, the diffraction peak intensity of free carbon becomes weak. When adding 30% and 40% ethylene glycol, with the increase of C content, resulting in the pyrolysis products of free

carbon and B_2O_3 distribution more uniform, the C and B_2O_3 reaction not completely, or the addition of C increased the molar ratio of C/B_2O_3 element in B_2O_3, the evaporation loss, so that C can not complete reaction. So the glycol dosage of 20%, under the temperature of 650 °C low-temperature pyrolysis at 1475 °C Celsius, reduction of 2.5 h B_4C obtained the best.

After the first cryogenic cracking, the organic precursor is lapping and then cracking 2 h at 700 °C and grinding into powder. The XRD diagram of the final product is obtained after the heat preservation at 1475 °C for 2.5 h. When the adding amount of ethylene glycol was 0% and 20% respectively, the final product of the corresponding XRD map in diffraction peaks of free carbon does not appear in the $2\theta = 23\text{-}27°$, $2\theta = 37.8°$ appeared only in the sharp peak characteristic diffraction peaks of B_4C. According to figure 3.9 to calculate the diffraction peak intensity ratio of B_4C and comparison, When the pyrolysis temperature second to 700 °C, adding 0% and 20% ethylene glycol, reduction temperature can be compared with pure B_4C at the same temperature, the crystallization degree of B_4C is the highest. At the same time, compared with not adding ethylene glycol, when the molar fraction of 20%, at $2\theta = 37.8°$ B_4C characteristic diffraction peaks of the higher intensity, indicating better crystallinity of B_4C.

SEM analysis

The pyrolysis products and free carbon washing with hot water to remove the B_2O_3 after SEM were analyzed. After the first organic precursor pyrolysis, grinding into powder, and then at a temperature of 650 °C cracking 2 h, get pyrolysis products. Through the analysis of pyrolysis products of surface water washing before and after SEM.

The pyrolysis products Fig. 5(a-e) and washing with hot water after the residue Fig. 5(f-j). The surface morphology can be found that the organic precursor through hot water washing, removing surface pyrolysis products of B_2O_3 on the surface of solid is obtained after the emergence of network structure with holes, which is characteristic of metastable structure of polymer blends and glass decomposition boroglyceride. Ester of boric acid and glycerol esterification is a transparent glass like solid, due to the cleavage of the B-O-C bond, decomposition state and metastable state similar to the decomposition of precursor heat, that is to say, in the air of the thermal decomposition reaction of B_2O_3 and carbide produced phase difference [22].

From the Fig. 5(a-e) can be seen, when not adding ethylene glycol, uneven surface cracking products. When adding ethylene glycol, the pyrolysis products becomes uniform surface, and with ethylene glycol content gradually increased, the surface cracking product gradually becomes uniform by uneven, when added to 40%, understand the product surface smooth.

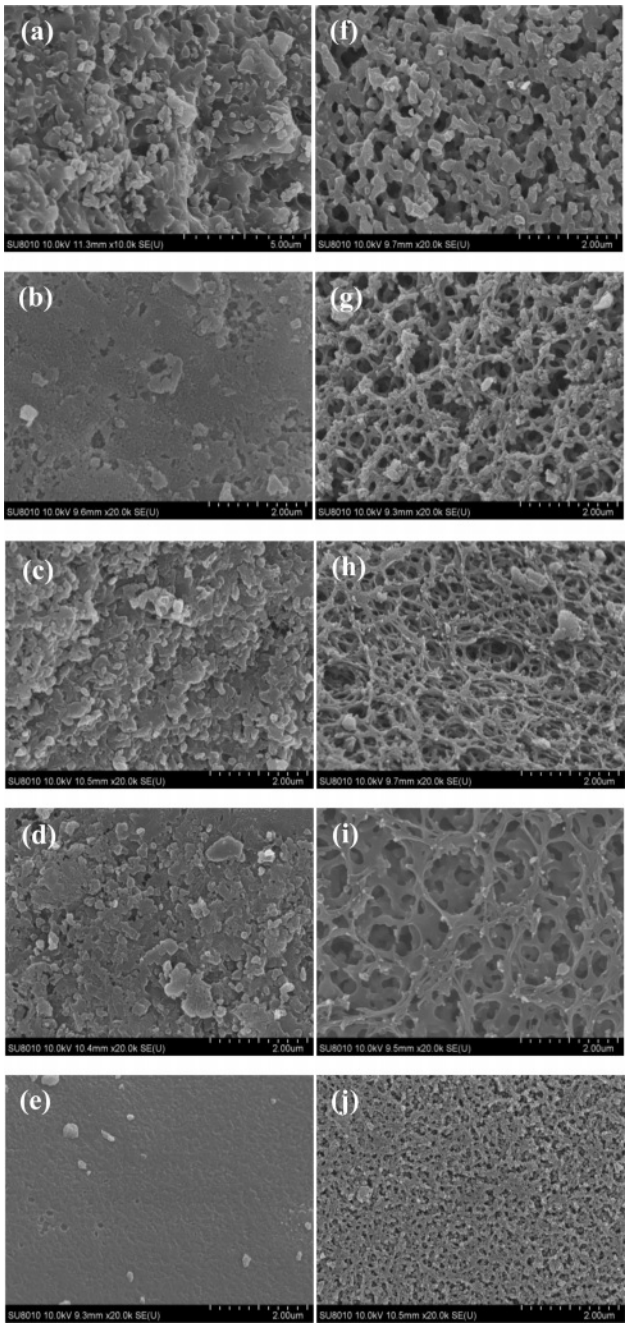

Fig. 5. SEM images of (a-e) precursor powders and (f-j) the carbon structure after hot water washed.

When the pyrolysis products were washed by Fig. 5(f-j) it can be seen that the amount of ethylene glycol is 0-30%, with hot distilled water dissolved in the pyrolysis products of B_2O_3, solid surface of the three-dimensional network structure continuous. When the adding amount of ethylene glycol is 20%, by Fig. 5(f) can be seen, heat into three-dimensional network structure of continuous pyrolysis of solid surface water after washing, pyrolysis products surface is the most uniform, the pore size of the pores on the surface of solid phase. The width of about 0.2 um, with two ethanol fraction B increases, the width of carbon structure Gradually become

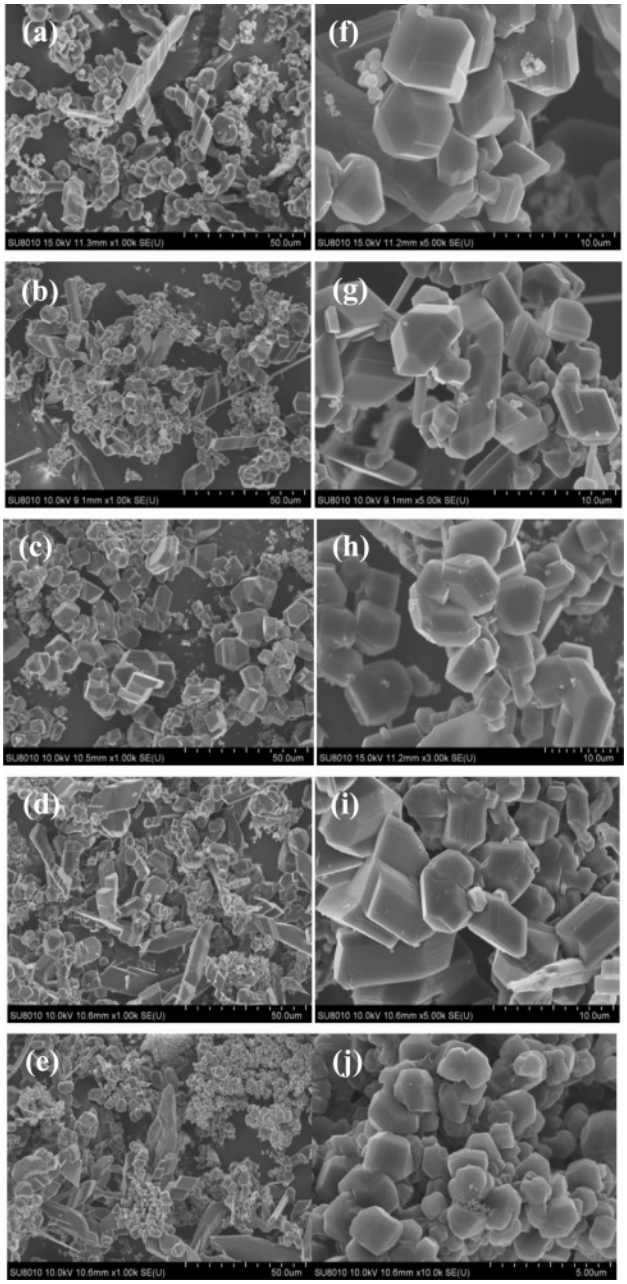

Fig. 6. SEM images of final products adding 0-40% mole of EG

smaller, in Fig. 5(h) carbon structure width less than 0.1 um. in the B_2O_3 network structure gap, its size is about 0.1-0.5 um. when the molar fraction of ethylene glycol is increased to 30%, the carbon structure appears on the surface of the size of the hole, and when the molar fraction of ethylene glycol. To 40%, the carbon surface structure no longer appear three-dimensional continuous network structure, indicating a large amount of ethylene glycol with ethylene glycol and glycerol boric acid for reaction, make a lot of surplus, thermal decomposition, pyrolysis products only a lot of sintered carbon, the B_2O_3 is not evenly distributed.

According to all of the pyrolysis products of SEM analysis can be found, when adding 20% glycol, after the first low temperature cracking, pyrolysis products are then second low temperature cracking at 650 ℃ after the free carbon network structure, complete, compact, solid surface pores of uniform size (Fig. 5(h)). At this time B_2O_3 in the best dispersion of free carbon.

Fig. 6 shows final product of 1000 times magnification (a-e) and 5000 times (f-j), boric acid-glycerol system added with 0-40% glycol. It keeps 2 h in air at 250 ℃. Then it keeps 2 h at 350 ℃, and finally cleavages 2 h at 650 ℃. After that, high purity argon is used as a protective gas, and then it is reduced to 2.5 h at 1475 ℃ high temperature, and the final product is obtained. Except for Fig. 6(e), there are other products in a large number of finished strip type massive crystal, dendrite, and small lamellae. Presumably by different reaction mechanisms the form. The bulk crystal is liquid B_2O_3 and free carbon liquid solid interfacial reaction formation. Because the raw material in the presence of a large number of carbon particle particle nucleation, it can be formed in the surface of carbon particle attachment, so that boron carbide nucleation mode for heterogeneous nucleation. And the carbon particle size of uniform. The growth rate of grain in each direction is consistent, so the bulk crystal [19]. It can form the Gestalt also suggested that the elongated dendrite is due to gaseous B_2O_3 and free carbon gas-solid interface reaction. Fig. 6(b) is a massive part of crystal, crystal is six angle diamond with particle size is about 3 um, which is irregular block. Fig. 6(j) can find that the blocky structure is incomplete and slightly agglomerate. With the increase of ethylene glycol, the agglomeration of the final products is more serious and the particle size is smaller. When the amount of ethylene glycol exceeds 20%, the carbon network structure becomes denser and denser, resulting in the subsequent addition of ethylene glycol to increase the grain size.

Conclusion

According to the infrared spectrum of the organic precursor, it is known that the esterification of boric acid to glycerol and glycol, respectively. According to the analysis of organic precursor TG results, the first low temperature pyrolysis of organic precursors was determined: first from room temperature to 250 ℃ keeping 2 h after heating, grinding, to remove the free water in the precursor; and then heated to 350 ℃ keeping 2 h heating, grinding into powder. The organic precursors were obtained after low temperature pyrolysis and two times of grinding. A mixture of free carbon and B_2O_3 was obtained. The free carbon surface showed a three-dimensional network structure, and B_2O_3 was distributed in the carbon network. The pyrolysis products of high temperature reduction as raw material, the higher reduction temperature, reduction time is longer, more conducive to the formation of boron

carbide. The greater the amount of ethylene glycol, the agglomeration of the final product more serious. When the adding amount of ethylene glycol is 20%, the pyrolysis products of 2.5 h reduction at 1475 ^{o}C, with hexahedral structure, average particle size of 3.089 um, the purity of B_4C powder for 92.89%.

Acknowledgement

The authors would like to acknowledge financial support from Key Laboratory of Liaoning Province for Polymer Catalytic Synthesis, Liaoning Provincial Engineering Laboratory for Advanced Polymeric Materials and High-tech Research and Development Project of Liaoning Provincial Industrial Special Resources Protection Office (Liao Cai Qi [2013]736).

References

1. V. Domnich, S. Reynaud, R.A. Haber, and M. Chhowalla, J. Am. Ceram. Soc. 94[11] (2011) 3605-3628.
2. N. Vast, J.M. Besson, S. Baroni, and A. Dal Corso, Comput. Mater. Sci. 17[2-4] (2000) 127-132.
3. M.M. Balakrishnarajan, P.D. Pancharatna, and R. Hoffmann, New J. Chem. 31[4] (2007) 473-485.
4. X. Chen, S. Dong, Y. Kan, H. Zhou, J. Hu, and Y. Ding, Rsc Adv. 6[11] (2016) 9338-9343.
5. A.M. Hadian and J.A. Bigdeloo, J. Mater. Eng. Perform. 17[1] (2008) 44-49.
6. L. Pei and J. Min, Nucl. Power Eng. 33[2] (2012) 110-113.
7. A. Alizadeh, E. Taheri-Nassaj, and N. Ehsani, J. Eur. Ceram. Soc. 24[10-11] (2004) 3227-3234.
8. L. Shi, Y. Gu, L. Chen, Y. Qian, Z. Yang, and J. Ma, Solid State Commun. 128[1] (2003) 5-7.
9. C. Suryanarayana, Prog. Mater. Sci. 46[56] (2001) 1-184.
10. N. Tahara, M. Kakiage, I. Yanase, and H. Kobayashi, J. Alloys Compd. 573[88] (2013) 58-64.
11. I. Yanase, R. Ogawara, and H. Kobayashi, Mater. Lett. 63[1] (2009) 91-93.
12. S. Mondal and A.K. Banthia, J. Eur. Ceram. Soc. 25[2-3] (2005) 287-291.
13. P.M. Barros, O.V.P. Yoshida, and M.A. Schiavon, J. Non. Cryst. Solids 352[32-35] (2006) 3444-3450.
14. Rafi-ud-dina, G.H. Zahid, E. Ahmad, M. Maqbool, T. Subhani, W.A. Syed, and S.Z. Hussain, J. Inorg. Organomet. Polym. 25[4] (2015) 995-999.
15. A. Sinha, T. Mahata, and B.P. Sharma, J. Nucl. Mater. 301[2-3] (2002) 165-169.
16. A.K. Khanra, Bull. Mater. Soc. 30[2] (2007) 93-96.
17. Rafi-ud-dina, G.H. Zahida, Z. Asghar, Muhammad Maqbool, E. Ahmada, T. Azhar, T. Subhani, and M. Shahzada, J. Asian Ceram. Soc. 2[3] (2014) 268-274.
18. M. Kakiage, N. Tahara, I. Yanase, and H. Kobayashi, Mater. Lett. 65[12] (2011) 1839-1841.
19. A. Najafi, F. Golestani-Fard, H.R. Rezaie, and N. Ehsani, Ceram. Int. 38[5] (2012) 3583-3589.
20. T.R. Pilladi, K. Ananthasivan, S. Anthonysamy, and V. Ganesan, J. Mater. Sci. 47[4] (2012) 1710-1718.
21. M. Kakiage, Y. Tominaga, I. Yanase, and H. Kobayashi, Powder Technol. 221[257-263] (2012) 25-263.
22. X. Chen, S. Dong, Y. Kan, H. Zhou, J. Hu, and Y. Ding, Rac. Adv. 6[11] (2016) 9338-9343.
23. S. Chuan, L. Xiaogang, C. Yunbo, Z. Lingli, and L. Yunkai, J. Ceram. Process. Res. 22[3] (2021) 340-344.
24. W. Hongkang, Z. Yujun, and D. Xiangyu, J. Ceram. Process. Res. 12[3] (2011) 599-601.
25. K.H. Kim, K.B. Shim, J.H. Chae, J.S. Park, and J.P. Ahn, J. Ceram. Process. Res. 10[6] (2009) 716-720.